A Priori Prediction of Propagation Rate Coefficients in Free-Radical Polymerizations: Propagation of Ethylene

Johan P. A. Heuts and Robert G. Gilbert*

School of Chemistry, University of Sydney, Sydney, NSW 2006, Australia

Leo Radom*

Research School of Chemistry, Australian National University, Canberra, ACT 0200, Australia

Received May 3, 1995; Revised Manuscript Received August 28, 1995[⊗]

ABSTRACT: A method is derived for calculating Arrhenius parameters for propagation reactions in free-radical polymerizations from first principles. Ab initio molecular orbital calculations are carried out initially to determine the geometries, vibrational frequencies, and energies of the reactants and the transition state. Transition state theory then yields the Arrhenius parameters. The lowest frequencies are replaced by appropriate (hindered or unhindered) internal rotors, to better model these modes in the calculation of frequency factors. It is found that a high level of molecular orbital theory (e.g., QCISD-(T)/6-311G**) is required to produce reasonable activation energies, whereas satisfactory frequency factors can be obtained at a relatively simple level of theory (e.g., HF/3-21G), because the frequency factor is largely determined by molecular geometries which can be reliably predicted at such a level. Obtaining reliable frequency factors for quite large systems is thus possible. The overall procedure is illustrated by calculations on the propagation of ethylene, and the results are in accord with literature experimental data. Means are also derived for extending the results from propagation of monomeric radicals to propagation of polymeric radicals, without additional computational requirements. The method is expected to be generally applicable to those propagation reactions that are not significantly influenced by the presence of solvent (i.e., relatively nonpolar monomers in nonpolar solvents). The calculations show that the magnitude of the frequency factor is largely governed by the degree to which the internal rotations of the transition state are hindered. They also suggest that there can be a significant penultimate unit effect in free-radical copolymerization. Furthermore, the calculations explain the rate-enhancing effect found upon deuteration of the monomers and explain why the rate coefficient for the first propagation step is larger than that for the long-chain propagation step.

Introduction

Kinetic modeling and mechanistic deductions in any chemical process require accurate rate coefficients. As has been noted previously,[1] accurate rate coefficients in free-radical polymerizations are difficult to establish. Whereas the experimental determination of the propagation rate coefficient (k_p) is relatively easy in the case of some monomers, e.g., styrene,[2] it is very difficult for other systems, e.g., acrylates.[3] A major cause of this problem is the fact that several reactions, e.g., propagation, transfer, and termination, are taking place simultaneously and that interpretation of experimental kinetic data is model dependent. In cases where the relative importance of the individual processes cannot be accurately assessed, the experimental results may be interpreted incorrectly and hence may lead to incorrect rate coefficients and mechanistic inferences. A theoretical understanding of the factors that govern the reaction rates and a model to predict the rate coefficients should lead to a better interpretation of the experimental data. It may then become possible to understand and predict, for example, more subtle effects such as the effects of deuteration of monomers and possible penultimate unit effects.

A possible way of approaching the problem is through transition state theory (TST), which has been successfully used previously for (semi)quantitative predictions in gas-phase reactions.[4,5] Earlier attempts to develop a model for the frequency factor of k_p, e.g., by Guaita,[6] used empirical parameters such as entropic group contributions, evaluated from a limited number of hydrocarbons, in the TST expressions. Guaita's model also requires the estimation of certain entropic effects due to conjugation, which is not straightforward in many cases. Although such models could be used for some qualitative predictions, the empirical parameters limit their applicability for general (semi)quantitative predictions. On the other hand, if the TST approach could be based only on the intrinsic fundamental properties of the reacting molecules, it would suffer less from such limitations and a more quantitative model would consequently be possible for an a priori estimation of rate coefficients.

At the simplest level, use of TST for the prediction of the rate coefficient of a reaction requires the geometry, vibrational frequencies, and relative energies in the reactants and the TS as input. In principle, these fundamental properties can be obtained experimentally for the reactants, but in practice this would be extremely difficult for radicals and virtually impossible for transition states.[7] Easily implemented and user-friendly theoretical procedures such as molecular mechanics[8] and semiempirical quantum chemical methods such as AM1[9] may yield reasonably good results for some properties, but it is uncertain whether they will yield adequate results for all the properties required to obtain accurate rate coefficients. Ab initio quantum chemistry can accurately predict properties such as geometries, frequencies, and energies provided that appropriate levels of theory are used.[10]

In this paper, propagation in the free-radical polymerization of ethylene is used as a case study. This system is of intrinsic interest but, in addition, is

[⊗] Abstract published in *Advance ACS Abstracts,* November 1, 1995.

0024-9297/95/2228-8771$09.00/0

sufficiently small so as to allow the use of high-level ab initio quantum chemical methods, which enables us to develop a general model with a minimum number of assumptions.

It is important to note that the calculations refer to gas-phase reactions. However, it is expected that the results will also be applicable to propagation reactions in solution. Radical–molecule transition states, as occur in free-radical polymerizations, are known to be usually relatively unaffected by the presence of solvent,[11] and indeed radical reactions in general are usually insensitive to solvent effects.[12] For this reason, one might suppose that the gas-phase calculations will provide quite good estimates of the rate coefficients for such reactions in condensed phases (e.g., in a polymerization medium).

Brief Overview of Transition State Theory

One of the fundamental concepts in chemical dynamics is the idea that atoms within molecules move according to forces derived from a potential field which is determined by electronic interactions. A description of the energy as a function of all possible coordinates of the atoms is called the potential surface and in principle can be obtained by quantum mechanical calculations. Solving the classical equations of motion on the potential surface yields the momenta and positions of all atoms at any time, i.e., a trajectory. An exact classical evaluation of the rate coefficient can be obtained by computing a large number of trajectories and averaging the velocities of the trajectories that start as reactants and end as products on the potential surface.[5]

The mathematics for the description of this process can be greatly simplified by making the *transition state assumption*.[5] In transition state theory (TST), it is assumed that there exists a critical geometry constraint on the potential surface such that all the trajectories passing through a geometry with this constraint originate as reactants and end as products (reactive trajectories). This critical geometry constraint could be the length of a forming C–C bond in a process such as propagation: in the reactants this length is infinite and in the product it is about 1.54 Å, so the constraint could be in the vicinity of 2 Å (i.e., any trajectory where the carbon atoms approach closer than 2 Å will react, no matter what the other atoms might do). The system with this constraint is called the transition state (TS) and the energy is usually a maximum on the reaction pathway between the reactants and products.

Evaluating the mathematical description of this process yields the relatively simple expression of eq 1:[4,5]

$$k_p = \frac{kT}{h}\frac{Q^\dagger}{Q_{mon}Q_{rad}}\exp\left(-\frac{E_0}{kT}\right) \tag{1}$$

which now does not depend on the complete potential surface, but only on the properties of the TS and reactants. In this TST expression for the propagation rate coefficient k_p, k is Boltzmann's constant, T is the temperature, h is Planck's constant, E_0 is the critical energy (i.e., the zero-point energy difference between reactants and transition state), and $Q^\dagger$, Q_{mon}, and Q_{rad} are the molecular partition functions for the TS, monomer, and radical, respectively. The Arrhenius frequency factor, A, and activation energy, E_{act}, can be related to the preexponential factor and critical energy in eq 1 by simple statistical thermodynamic relationships.[4,5] For the frequency factor, the following expression can be derived:

$$A = \frac{ekT}{h}\exp\left(\frac{\Delta S^\ddagger}{k}\right) \tag{2}$$

where e is the base of the natural logarithm and $\Delta S^\ddagger$ is the entropy of activation, which is simply related to the molecular partition functions by the following relation:

$$\Delta S^\ddagger = k\ln\left(\frac{Q^\dagger}{Q_{mon}Q_{rad}}\right) - \frac{k}{T}\frac{\partial\ln\left(\frac{Q^\dagger}{Q_{mon}Q_{rad}}\right)}{\partial T^{-1}} \tag{3}$$

The activation energy is given by

$$E_{act} = E_0 - k\frac{\partial\ln\left(\frac{Q^\dagger}{Q_{mon}Q_{rad}}\right)}{\partial T^{-1}} + kT \tag{4}$$

As can be seen from eqs 3 and 4, it is necessary to know the molecular partition functions in order to evaluate the frequency factor and activation energy.

Usually, the Hamiltonians of the reactants and transition state are assumed to be separable, in which case the molecular partition function Q can be written as a product of translational, vibrational, and rotational terms:[13]

$$Q = Q_{trans} \times Q_{vib} \times Q_{rot} \tag{5}$$

Here, it is assumed that the reaction occurs on a single electronic surface, which is indeed the case in the present system: reactants (i.e., the radical and monomer), transition state, and product (i.e., the radical increased by one monomer unit) all belong to the same (doublet) state.

In the following sections, the separate contributions to the frequency factor of propagation reactions in general will be discussed in more detail.

(a) Translational Partition Function. The translational partition function of an ideal gas molecule is given by

$$Q_{trans} = V\left[\frac{2\pi mkT}{h^2}\right]^{3/2} \tag{6}$$

where V is the reference volume and m is the mass of the translating molecule. In the case of a radical addition reaction, the translational contribution to the frequency factor is then given by

$$\left[\frac{Q^\dagger}{Q_{mon}Q_{rad}}\right]_{trans} = \frac{1}{V}\left[\frac{m_{mon}+m_{rad}}{m_{mon}m_{rad}}\right]^{3/2}\left[\frac{h^2}{2\pi kT}\right]^{3/2} \tag{7}$$

The long-chain limit for the propagation reaction has $m_{rad} \approx m^\dagger$, so eq 7 will then reduce to

$$\left[\frac{Q^\dagger}{Q_{mon}Q_{rad}}\right]_{trans}^{\text{long chain}} \approx \frac{1}{V}\left[\frac{1}{m_{mon}}\right]^{3/2}\left[\frac{h^2}{2\pi kT}\right]^{3/2} \tag{8}$$

As is clear from eq 8, different monomers will have different translational contributions to the frequency factor if their masses are different. For example, changing the monomer from ethylene to butyl methacrylate decreases this contribution by a factor of approximately 10.

(b) Vibrational Partition Function. The vibrational partition function for the ith harmonic oscillator is given by

$$Q_{\text{vib},i} = \left[1 - \exp\left(-\frac{h\nu_i}{kT}\right)\right]^{-1} \tag{9}$$

where ν_i is the frequency. For a polyatomic molecule, the vibrational partition function is for practical purposes approximated as the product of the vibrational partition functions of separate vibrational modes:

$$Q_{\text{vib}} = \prod_i Q_{\text{vib},i} \tag{10}$$

In principle, the fundamental frequencies of the reactants can be obtained by experiment, but in general they are very difficult to obtain for radicals and experimentally unattainable for transition states. Experimental infrared data for radicals are very scarce and the low frequencies, which have the largest contributions to the frequency factor (see eq 9), are often not reported.[14] Quantum chemical calculations provide an alternative means of reliably determining the fundamental vibrational frequencies, both for reactants and for transition states.[10] Moreover, since the TST expression contains the *ratio* of partition functions, it is highly desirable that the frequencies of the reactants and of the TS be obtained by the same method, suggesting that theory has a useful role to play.

Not all the vibrations are taken into account in calculating the vibrational partition function. In the first place, the TS has one imaginary frequency (which is a characteristic of the TS), which corresponds to a motion along the reaction coordinate; this frequency is omitted from the partition function.[5] Furthermore, the actual motions of some low frequencies, as indicated by a normal-mode analysis, are better represented as internal rotations[15] and should be treated as either hindered or unhindered rotors (depending on the barrier to rotation). These frequencies are then omitted from the vibrational partition function and enter the rotational partition function. The value that we have chosen as an upper limit to treat these particular low-frequency modes as rotors is 200 cm^{-1}. Fueno and Kamachi[16] found that treating the methyl torsion as an unhindered one-dimensional rotor in the addition of a methyl radical to ethylene (~120 cm^{-1}) yields results very similar to those obtained by treating this mode as a harmonic oscillator. However, as will be shown in the following sections, this is not the case in general.[5]

A detailed examination of the vibrational modes in the TS and the reactants shows that there are 6 (1 imaginary and 5 real) extra modes in the TS which did not exist in the reactants. These modes, the so-called transitional modes, arise due to the loss of external translations and rotations of the reactants, when brought together in the TS.[5] All the other modes in the TS correspond to modes in the reactants and will have frequencies similar to the corresponding modes in the reactants (they will be slightly lower because of the higher mass of the TS). Because of the ratio $Q^\dagger/(Q_{\text{mon}}Q_{\text{rad}})$ in the above relations, this implies that the total vibrational contribution is mainly determined by the frequencies of the 5 real transitional modes. These frequencies typically lie below 1000 cm^{-1} and the lowest frequencies mostly correspond to torsional modes. In the case of n-alkyl radical additions to ethylene, it will be seen that the transitional modes lie between roughly 40 cm^{-1}, corresponding to an internal rotation, and 650 cm^{-1}. If the torsional modes below 200 cm^{-1} are properly treated as hindered rotors, it may be assumed that the remaining contributions arise from harmonic oscillators with frequencies greater than approximately 100 cm^{-1}, with the majority of them in the range of 200–700 cm^{-1}. These frequencies lead to values of the vibrational partition functions from 2.8 (ν = 100 cm^{-1}) to 1.05 (ν = 700 cm^{-1}) at 323 K. Hence, the overall vibrational contribution to the frequency factor will have a value typically between 1 and 10:

$$1 < \left(\frac{Q^\dagger}{Q_{\text{mon}}Q_{\text{rad}}}\right)_{\text{vib}} < 10 \tag{11}$$

Since the TS's of the propagation reactions of different monomers will all have similar characteristics, the differences in the overall vibrational contributions (after removing the hindered rotations) will be small. Sterically more crowded monomers will probably show an increase in the frequency of a particular mode as compared with a similar mode in a less crowded monomer. However, even an extremely large increase in frequency from 200 to 600 cm^{-1} only results in a decrease in the overall vibrational contribution by a factor of 1.6. We may thus conclude that the vibrational contribution to the frequency factor shows little variation from system to system.

(c) Rotational Partition Function. This partition function, which has both external and internal rotation components, is that component of the frequency factor which can vary most strongly from sytem to system. All (nonlinear) molecules exhibit an external three-dimensional rotation, for which the partition function is given by

$$Q_{\text{ext rot}} = \frac{\pi^{1/2}}{\sigma}\left(\frac{8\pi^2 kT}{h^2}\right)^{3/2}(I_a I_b I_c)^{1/2} \tag{12}$$

where σ is the symmetry number of the molecule and I_a, I_b, and I_c are the principal moments of inertia, given by $I = \sum m_i r_i^2$, where m_i and r_i are the mass and the distance to the appropriate principal axis of rotation, respectively, of atom i. The principal moments of inertia can be easily calculated if the geometry of the molecule is known. In the case of a small radical adding to the monomer, the external rotations of both reactants and the transition state have to be considered, but in the long-chain limit of the propagation reaction, it is only the external rotation of the monomer that is important (since the moments of inertia of the macroradical and the TS will not differ significantly and will approximately cancel in eq 1), leading to

$$\left(\frac{Q^\dagger}{Q_{\text{mon}}Q_{\text{rad}}}\right)_{\text{ext rot}}^{\text{long chain}} \approx \left(\frac{1}{Q_{\text{mon}}}\right)_{\text{ext rot}} \tag{13}$$

While the values of a vibrational partition function are of order unity, those of $Q_{\text{ext rot}}$ are of the order 10^2–10^4.

As stated in the previous section, internal rotations have to be taken into account if low vibrational frequencies are present in the molecule. Internal rotations may be described as hindered one-dimensional[17–20] or two-dimensional[5] rotors. Pitzer[18] has tabulated the values for the rotational partition functions of one-dimensional rotors for which the rotational potential is given by a single cosine function, and some very useful analytical approximations to these tables were published by Troe[19]

and Truhlar.[20] The main disadvantage of these methods is that they can only be applied to potentials given by a single cosine and, as will be shown in a later section, many potentials cannot be approximated by a single cosine function. A way around this problem is to calculate the energy levels of the rotational potential by solving the appropriate one-dimensional Schrödinger equation:[13]

$$-\frac{h^2}{8\pi I_r}\frac{\partial^2\Psi}{\partial\theta^2} + V(\theta)\Psi = \epsilon\Psi \qquad (14)$$

where I_r is the reduced moment of inertia, $V(\theta)$ is the potential energy at a given torsion angle θ, Ψ is the wavefunction, and ϵ is the corresponding energy of the system. The partition function can then be calculated by directly counting the energy levels according to[13]

$$Q_{\text{int rot}} = \frac{1}{\sigma_{\text{int}}}\sum_i \exp\left(-\frac{\epsilon_i}{kT}\right) \qquad (15)$$

where ϵ_i is the energy of level i and σ_{int} is the symmetry number of the internal rotation. This partition function typically has a value lying between 1 and 10. Since both steric and mass effects are explicitly taken into account in the internal rotational partition function, it is often the dominating factor that determines the differences in frequency factors for different monomers.

Computational Procedures

Standard ab initio molecular orbital procedures[10] have been used to determine the geometries, harmonic vibrational frequencies, and energies of the reactants and transition states. Geometry optimizations were performed at the HF/3-21G, HF/6-31G*, and MP2/6-31G* levels of quantum chemical theory.[10] The vibrational frequencies of the optimized structures and the rotational barriers were also calculated at these levels. Reaction barrier calculations were performed at higher levels of theory, up to QCISD(T)/6-311G**.[21] Calculations on ethylene were performed with the restricted Hartree–Fock (RHF) or Møller–Plesset (RMP) procedures, whereas all the open-shell systems were treated with the unrestricted Hartree–Fock (UHF) or Møller–Plesset (UMP2) procedures. The symbols R and U are dropped for simplicity in the remainder of this paper. All calculations were carried out with the GAUSSIAN 92 software package;[22] details of the calculations will be reported elsewhere.[23]

The energy levels of the hindered rotations were calculated by solving the one-dimensional Schrödinger equation (eq 14), using the finite element method[24] extended to handle cyclic boundary problems.[25] A basis set of free rotor functions, ϕ_m, given by

$$\phi_m = \frac{1}{(2\pi)^{1/2}}\exp(im\theta) \qquad (16)$$

was used, where m is an integer between −200 and +200. Rotational potentials were determined by fitting a three-term Fourier expansion through the stationary points of the potential.

Calculations of the rotational constants ($=h^2/8\pi^2 I$) required to obtain the partition functions of the internal rotations were performed with GEOM, a part of the UNIMOL software package.[26] For this purpose, we used the optimized structures obtained by the ab initio calculations while the low-frequency torsions were treated as rigid rotors about specific bonds.

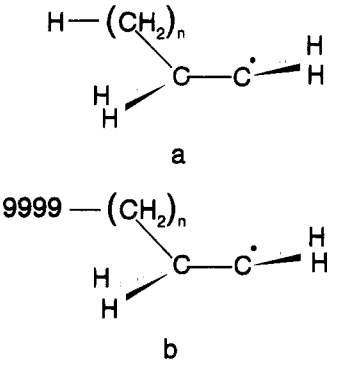

Figure 1. Schematic representation of (a) the radicals and (b) the corresponding "macroradicals" examined in this study (n = 0–5).

Simulations of the polymeric free radical and TS were performed by replacing the outermost trans hydrogen in the radical by a sphere with mass 9999 amu ("macroradicals"), as depicted in Figure 1. Calculations were carried out for the addition to ethylene of radicals ranging from ethyl radical to n-heptyl radical and of their corresponding "macromolecules".

Normal mode analyses of isotopically substituted molecules were performed using the original force constants and the masses of the new isotopes.

Results and Discussion

Reactants. The geometry of ethylene was optimized and vibrational analyses were performed at the HF/3-21G, HF/6-31G*, and MP2/6-31G* levels of theory. A lowest frequency of 897.2 cm^{-1} (HF/6-31G*) was found, which is sufficiently large that no attention is required with respect to internal rotations in ethylene. All radicals (i.e., ethyl, n-propyl, n-butyl, n-pentyl, n-hexyl, and n-heptyl) were optimized in the extended conformation (C_s symmetry) at the HF/3-21G and HF/6-31G* levels of theory. The ethyl, n-propyl, and n-butyl radicals were also optimized at the MP2/6-31G* level of theory. Vibrational analyses showed a normal mode with a frequency below 200 cm^{-1} corresponding to the methylene (CH_2) rotation at the radical terminus for all the radicals considered. For radicals larger than the ethyl radical, additional low-frequency modes occur, due to skeletal vibrations. In the cases of hexyl and heptyl radicals, these frequencies even drop below the frequency of the CH_2 rotation. However, these skeletal vibrations hardly change in going from reactants to the TS and their contributions will approximately cancel in the TST expression. These modes were therefore described for simplicity as harmonic oscillators.

Examination of the CH_2 torsion in more detail shows that it corresponds to a combination of a rotation of the CH_2 group and an inversion at the radical center. It is schematically represented for the case of the ethyl radical in Figure 2. The starting minimum energy conformation (I) has a nonplanar CCH_2 arrangement. Inversion at the radical center leads, via the maximum energy conformation II in which the CCH_2 group is planar, to conformation III (which is equivalent to I). A second inversion via conformation IV (which is equivalent to II) requires motion of the second hydrogen at the radical center.

Stationary points for this motion in the ethyl and propyl radicals were determined at the HF/3-21G, HF/

Table 1. V_i Values (kJ mol^{-1}) at the HF/3-21G, HF/6-31G*, and MP2/6-31G* Levels of Theory[a]

		CH_2 torsion in radical			C_2H_4 torsion in TS		C_3H_6 torsion in TS	
	V_i[b]	$C_2H_5^\bullet$	$C_3H_7^\bullet$	V_i[c]	$C_2H_5^\bullet$	$C_3H_7^\bullet$	$C_2H_5^\bullet$	$C_3H_7^\bullet$
HF/3-21G	V_2	0	0.07	V_1	−0.39	−0.17	0.00	−9.69
	V_4	0	−0.07	V_2	−0.19	−0.28	0.00	−5.30
	V_6	0.39	0.53	V_3	−3.33	−3.12	−6.82	−9.47
HF/6-31G*	V_2	0	−0.85	V_1	0.00	−0.01	0.00	−9.45
	V_4	0	−0.16	V_2	−0.27	−0.44	0.00	−5.14
	V_6	0.71	0.83	V_3	−3.64	−3.49	−7.73	−9.76
MP2/6-31G*	V_2	0	−0.84	V_1	1.86	2.03	0.00	−8.62
	V_4	0	−0.28	V_2	−0.25	−0.50	0.00	−5.65
	V_6	0.71	0.74	V_3	−3.93	−3.66	−6.84	−9.11

[a] For details, see ref 23. [b] From eq 17. [c] From eq 18.

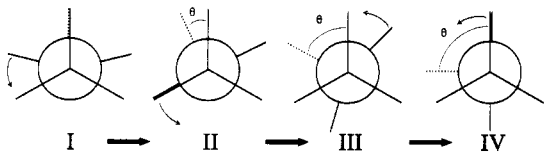

Figure 2. Schematic representation of the CH_2 rotation–inversion process in the ethyl radical involving the sequential movement of the two hydrogens at the radical center. The dihedral angle θ defines the coordinate for this mode.

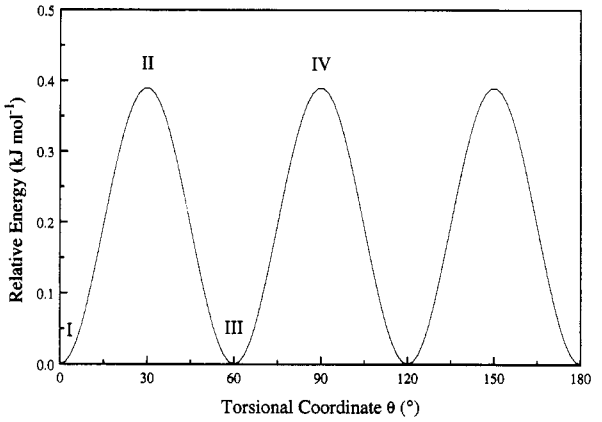

Figure 3. Potential energy profile for the CH_2 torsion in the ethyl radical at the HF/3-21G level of theory, without ZPVE corrections. The torsional coordinate θ and the structures corresponding to the stationary points are defined in Figure 2.

6-31G*, and MP2/6-31G* levels of theory. Since all radicals were optimized in completely extended conformations, the CH_2 rotational potentials for larger radicals are assumed in the rate calculations to be the same as those for propyl. The potentials were fitted by the truncated Fourier series

$$V(\theta) = \frac{1}{2}[V_2(1 - \cos 2\theta) + V_4(1 - \cos 4\theta) + V_6(1 - \cos 6\theta)] \quad (17)$$

and the values for the V_i are given in Table 1. The low barriers for the CH_2 rotation indicate a virtually unhindered rotation at 323 K (RT = 2.7 kJ mol^{-1}).

In Figure 3, the rotational potential for the CH_2 torsion in the ethyl radical is shown, and it can be seen that there are six identical wells in the potential (0–360°), giving rise to a symmetry number of 6 for this rotation. However, it is not clear that a symmetry number of 6 is entirely appropriate if we consider the actual geometries of the two stationary conformations of the ethyl radical: the minimum energy conformation (I) has a symmetry number of 3 for a rigid CH_2 rotation because of the nonplanarity of the radical carbon center, whereas the maximum energy conformation (II) has a symmetry number of 6. In the light of the actual form of the potential, we chose a symmetry number of 6 for the ethyl radical and for consistency reasons a symmetry number of 2 for the propyl and larger radicals.

Table 2. Calculated Rotational Constants (cm^{-1}) for the "Methylene" Rotation in Several *n*-Alkyl Radicals and Their Corresponding "Macroradicals"

	rotational constant[a]	
	radical	"macroradical"
ethyl	32.90	35.28
propyl	30.58	28.58
butyl	28.30	28.29
pentyl	28.15	27.95
hexyl	27.85	27.85
heptyl	27.83	27.75

[a] Optimized HF/3-21G geometries.

Rotational constants for this internal rotation in the radicals and their corresponding "macroradicals" are listed in Table 2. It can be seen from this table that from butyl onward, the rotational constant for the "macroradical" is almost the same as for the radical itself. In other words, the mass effect of the heavy atom, i.e., the simulated polymer chain, becomes smaller upon extending the chain length. Furthermore, it may be concluded that the butyl radical (i.e., a dimer in this case) contains the major overall rotational constant effects required for a reasonable description of the polymeric radical.

Transition States. Transition states were optimized and vibrational analyses were performed again at the HF/3-21G and HF/6-31G* levels of theory (with the transition states for the ethyl and *n*-propyl radical additions to ethylene also being studied at MP2/6-31G*). The optimized structure of the butyl radical + ethylene TS and its three most important low-frequency modes (<200 cm^{-1}) are depicted in Figure 4.

In all optimized TS structures, the lowest real frequency (ν_1 in Figure 4) is the internal rotation about the forming C–C bond, corresponding to ethylene rotation, and arises from the loss of one of the external rotations in the reactants when they are brought together in the TS. This mode is one of the five real transitional modes. The frequency for this mode drops from 59.1 to 33.7 cm^{-1} (HF/6-31G*) in going from the ethyl radical + ethylene TS to the heptyl radical + ethylene TS. These frequencies are not used in the frequency factor calculations, because these modes are replaced by internal rotations, for which the required rotational constants are calculated from the optimized TS geometry and the rotational potentials determined from the relevant stationary points on the potential energy surface. Rotational constants for this internal rotation are listed in Table 3. Again, it can be seen that

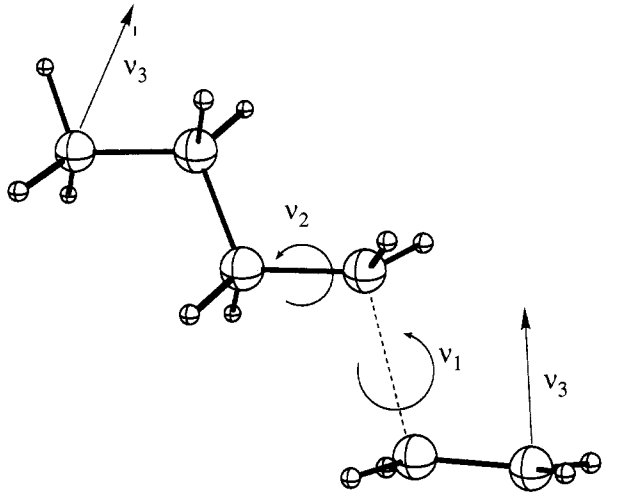

Figure 4. Optimized structure of the transition state for the addition of butyl radical to ethylene and its three most important low-frequency modes: ν_1, a transitional mode corresponding to the rotation of the "ethylene" group, ν_2, corresponding to the rotation of a "propylene" group, and ν_3, a transitional mode corresponding to a bending of the two bond angles of the forming C−C bond.

Table 3. Calculated Rotational Constants (cm^{-1}) for the "Ethylene" Rotation in the Transition States for the Addition of Ethylene to Several *n*-Alkyl Radicals and Their Corresponding "Macroradicals"

	rotational constant[a]	
	radical addition	"macroradical" addition
ethyl	8.33	6.18
propyl	5.87	5.86
butyl	5.72	5.52
pentyl	5.45	5.45
hexyl	5.40	5.31
heptyl	5.29	5.29

[a] Optimized HF/3-21G geometries.

the calculated rotational constants for the radical + ethylene TS and corresponding "macroradical" + ethylene TS are almost the same from butyl onward. The rotational potentials are fitted by

$$V(\theta) = \frac{1}{2}[V_1(1 - \cos\theta) + V_2(1 - \cos 2\theta) + V_3(1 - \cos 3\theta)] \quad (18)$$

and the values for the V_i are included in Table 1. The parameters for the propyl radical + ethylene TS are used for the description of the rotational potentials for all larger TS's, as in the case of the corresponding reactant radicals.

The second lowest frequency (ν_2 in Figure 4) corresponds to the rotation of a "propylene" moiety, consisting of the CH_2 group at the radical terminus and the ethylene group. This mode corresponds to the methylene rotation in the reacting radical; i.e., it is not a transitional mode. The frequency for this mode drops from 185.6 to 44.0 cm^{-1} (HF/6-31G*) in going from the ethyl radical + ethylene TS to the heptyl radical + ethylene TS. Again, this mode is best represented as an internal rotation, and the calculated values of the V_i (in eq 18) are included in Table 1. We note that the V_i values in larger TS's are assumed to be the same as for the propyl radical + ethylene TS. Rotational constants for this mode are listed in Table 4, from which it can be seen that for the butyl and larger radical additions the rotational constants for the "macroradical" + ethylene TS are almost the same as for the radical + ethylene TS, as was the case for the other internal rotations described above.

Table 4. Calculated Rotational Constants (cm^{-1}) for the "Propylene" Rotation in the Transition States for the Addition of Ethylene to Several *n*-Alkyl Radicals and Their Corresponding "Macroradicals"

	rotational constant[a]	
	radical addition	"macroradical" addition
ethyl	6.36	8.75
propyl	4.15	2.15
butyl	1.86	1.86
pentyl	1.72	1.51
hexyl	1.45	1.45
heptyl	1.40	1.31

[a] Optimized HF/3-21G geometries.

Table 5. Calculated HF/6-31G* Vibrational Frequencies (cm^{-1}) for the *n*-Butyl Radical to Ethylene Addition

	frequencies
ethylene	897.2, 1095.2, 1099.5, 1155.0, 1352.6, 1496.8, 1610.2, 1856.1, 3320.5, 3343.8, 3394.2, 3420.3
n-butyl (C_s symmetry)	131.0, 135.4, 259.5, 273.4, 414.5, 537.6, 783.9, 863.6, 941.7, 1025.2, 1092.5, 1137.0, 1191.7, 1310.6, 1403.5, 1423.2, 1451.7, 1522.7, 1564.1, 1602.8, 1633.9, 1639.1, 1643.5, 1653.7, 3186.8, 3196.3, 3198.7, 3210.7, 3232.0, 3260.9, 3261.4, 3307.3, 3404.1
TS (C_s symmetry)	458.4 (imaginary), 46.3, 71.7, 100.0, 135.5, 247.4, 260.8, 319.4, 401.4, 444.8, 633.0, 786.9, 789.3, 857.5, 883.7, 902.2, 944.8, 1017.6, 1033.2, 1045.4, 1092.7, 1135.7, 1208.9, 1277.2, 1322.7, 1339.4, 1410.1, 1430.9, 1454.4, 1528.1, 1564.1, 1595.8, 1613.4, 1633.5, 1639.3, 1643.7, 1654.0, 1673.6, 3183.9, 3193.8, 3197.9, 3206.5, 3228.7, 3260.1, 3260.8, 3280.4, 3316.1, 3327.7, 3361.3, 3393.4, 3418.7

The final significant low-frequency mode is a "bending" mode of the two reacting moieties in the TS (ν_3 in Figure 4), which has a value of 178.0 cm^{-1} for the ethyl radical + ethylene TS and drops to 57.4 cm^{-1} for the heptyl radical + ethylene TS. This mode also arises as a result of the loss of rotational degrees of freedom in the reactants and represents a second transitional mode. Due to its complexity and the high barriers for a significant bending of the important angles, this mode appears to be better represented as a harmonic oscillator and it was treated accordingly. The three remaining real transitional modes all have frequencies greater than 200 cm^{-1} and are therefore treated as harmonic oscillators.

As has been mentioned already, additional low-frequency modes are introduced upon extending the chain length, but these will be canceled in the frequency factor expression by the corresponding modes in the reacting radicals (see Table 5). They are therefore of minor importance in the evaluation of the rate coefficient and were treated as simple harmonic oscillators.

Frequency Factor Calculations. Frequency factors were calculated by numerical differentiation of eq 1. The treatment, as stated, assumes a complete separability of the Hamiltonian for the vibrational and rotational modes. The rotational potentials of the internal rotations were determined by complete optimization of the stationary points on the potential energy surface and fitting a three-term Fourier expansion to

Table 6. Calculated Frequency Factors (dm^3 mol^{-1} s^{-1}) for the Addition of the Ethyl Radical and Its Corresponding "Macroradical" to Ethylene at the HF/3-21G, HF/6-31G*, and MP2/6-31G* Levels of Theory (T = 323 K)

	frequency factor	
	$C_2H_5^\bullet + C_2H_4$	"macro-$C_2H_5^\bullet$" + C_2H_4
HF/3-21G	1.72×10^8	6.78×10^6
HF/6-31G*	1.91×10^8	8.35×10^6
MP2/6-31G*	1.29×10^8	5.68×10^6

these points, leading to the V_i listed in Table 1. By doing this, other motions are mixed into the rigid rotation, thus violating the assumption that the Hamiltonian is completely separable. However, the error introduced here is probably smaller than the error that would have been introduced by using a potential obtained by a rigid rotation; the latter would, for example, lead to rotational barriers that are significantly too high. For frequency factors involving the ethyl radical, the V_i from the ethyl calculations were used, whereas the propyl results were used for the frequency factors involving the propyl and all larger radicals.

Values for the frequencies for "macroradicals" were recalculated from the original force constants, but including the mass of the heavy atom. The contributions to the frequency factor of the translational and external rotational partition functions are essentially limited to the monomeric contribution (see eqs 8 and 13), because the mass and geometry of an infinitely long radical chain and its corresponding TS do not differ significantly.

First, we compare the frequency factors obtained with parameters from the three different quantum chemical methods in order to investigate whether convergence of the results occurs with increasing level of theory. The results for the addition of the ethyl radical to ethylene and the corresponding "macroradical" addition are listed in Table 6. It can be seen that the calculated values at the three levels of theory lie within a 30% range. This result can be understood by noting that geometries and vibrational frequencies, the main quantities required to calculate frequency factors, can be obtained reasonably accurately at relatively simple levels of theory. The differences in the optimized geometries at the HF/3-21G and MP2/6-31G* levels of theory do not lead to significant differences in the rotational constants for internal and external rotations.[10] This leads to external rotational contributions to the frequency factor of 2.3×10^{-2} (HF/3-21G), 2.3×10^{-2} (HF/6-31G*), and 2.2×10^{-2} (MP2/6-31G*) and internal rotational contributions to the frequency factor of 18.8 (HF/3-21G), 17.5 (HF/6-31G*), and 15.6 (MP2/6-31G*). Vibrational frequencies calculated at the HF/3-21G, HF/6-31G*, and MP2/6-31G* levels of theory are systematically too large by up to about 15% as compared with experiment,[27,28] and we have therefore scaled them by factors of 0.95, 0.89, and 1.00,[29] respectively, before use. The resulting vibrational contributions to the frequency factors are 3.2 (HF/3-21G), 3.5 (HF/6-31G*), and 3.1 (MP2/6-31G*); i.e., they lie within a 10% range. A more complete description of the scaling factor dependence of the calculated frequency factor is presented in the sensitivity analysis section of this paper (see below).

Having established that reasonable geometries and vibrational frequencies can be obtained at the HF/3-21G level of theory, we conclude that this method will be useful for larger monomer systems for which higher level calculations are not feasible. Frequency factors

Table 7. Comparison of Calculated (HF/3-21G) and Experimental[a] Frequency Factors (dm^3 mol^{-1} s^{-1}) for n-Alkyl Radical Additions to Ethylene (T = 323 K)

	frequency factor	
	calcd	exptl
ethyl	1.7×10^8	2.0×10^8
propyl	8.7×10^7	2.0×10^7
butyl	9.8×10^7	2.3×10^7
pentyl	7.9×10^7	
hexyl	6.3×10^7	
heptyl	5.0×10^7	

[a] See ref 12c.

Table 8. Convergence of Calculated Frequency Factors (dm^3 mol^{-1} s^{-1}) for the "Macroradical" Addition to Ethylene (HF/3-21G, T = 323 K)

"macroradical"	freq factor	"macroradical"	freq factor
ethyl	6.8×10^6	pentyl	2.7×10^7
propyl	1.2×10^7	hexyl	2.0×10^7
butyl	1.7×10^7	heptyl	1.6×10^7

calculated using HF/3-21G parameters for several alkyl radical additions in the gas phase are compared with literature data in Table 7. It can be seen that they are in reasonable agreement (given that the error in the experimental frequency factors is typically 50% for such systems), indicating a satisfactory description of the physics of the reacting system.

Using the same approximations as in the case of ethyl radical addition to ethylene, the frequency factors were calculated for the corresponding "macroradical" additions. From Table 8, it can be seen that the frequency factor moves toward a value in the range of $(1.0-1.7) \times 10^7$ dm^3 mol^{-1} s^{-1}, which is within the experimental uncertainty:[30,31] $0.9 \times 10^7 < A_{exp} < 1.9 \times 10^7$ dm^3 mol^{-1} s^{-1}. It is clear that the larger radicals are better models for the polymeric radical because the main error in our "macroradical" treatment occurs in the internal rotational partition function, which is a function of the moment of inertia. The error introduced here by replacing the hydrogen atom in the ethyl radical by a heavy mass is obviously greater than for the larger radicals, where most of the atoms are further away from the axes of rotation, as in real polymers. It can also be concluded that the butyl radical is already quite a good model for the simulation of the polymeric radical. This result also implies that if the properties of the dimeric radical are known, reasonable estimates can be made for the polymeric radical.

At this point, it is important to examine in more detail the difference between the calculated frequency factor for the ethyl radical addition and corresponding "macroradical" addition. The value for the "macroradical" addition is smaller by a factor of about 25, as can be estimated from eqs 8 and 13. In the first place, elimination of the masses of the radical and the transition state will reduce the total translational contribution in the preexponential factor in eq 1 by a factor of about 3 (the mass dependence reduces from about $(2m_{mon}/m_{mon}^2)^{3/2}$ in eq 7 to $(1/m_{mon})^{3/2}$ in eq 8). In addition, the total external rotational contribution is reduced by the factor $Q^{\dagger}_{ext\ rot}/Q_{rad,ext\ rot}$, which is approximately 15 in the case of the ethyl radical addition to ethylene. These two effects, which together lower the frequency factor by a factor of approximately 45, are partially canceled by an increase in the vibrational contribution to the frequency factor for the "macroradical" addition by about 40% due to the mass effect on the vibrational frequencies.

From a physical point of view, these "loss" factors can be explained as follows. Due to the overall rigidity of the long polymeric radical and the corresponding TS, we may assume that the external rotations and translations of these large species are of minor importance as compared with the very fast motions of the monomer on the time scale of the reaction. Therefore, the external rotational and translational contributions to the frequency factor of the polymeric radical and TS are negligible as compared with those of the monomer. This result thus supports the idea that the rate coefficient for the first propagation step (k_p^1) is larger than that for the propagation of polymeric radicals (k_p).[32] This will, however, be less than the factor of 25 because, as was shown, the "macroradical" based on the ethyl radical is not yet a good model for the polymeric radical. Many frequencies and rotational constants will be slightly lowered, which leads to a partial compensation of the overall "loss" factor. A better estimate for the difference between k_p and k_p^1 obtained as a consequence of the change in frequency factors is the difference between the results for the "macroheptyl" and the ethyl radical additions, which gives $k_p^1 \approx 10 \times k_p$ (see Tables 7 and 8).

Activation Energies. In the previous sections, attention was paid to the frequency factor for the propagation rate coefficient and it was concluded that the use of the relatively simple HF/3-21G level of quantum chemical theory is sufficient for its determination to reasonable accuracy. This, however, is not the case for the activation energy of the reaction, which is the other component of the propagation rate coefficient. High-level calculations have to be performed in order to obtain accurate relative energies of the reactants and transition state.[33,34] Activation energies obtained at the Hartree–Fock level of theory may not be reliable because the effect of electron correlation in calculating reaction barriers is generally important. In addition, the consequence of so-called spin contamination can be damaging.[34] We find that the activation energy for the addition of the ethyl radical to ethylene increases from 37.3 to 51.1 kJ mol^{-1} upon increasing the basis set from 3-21G to 6-31G* at the HF level of theory. Extending the basis set should give better and more reliable results, but the value of 51.1 kJ mol^{-1} is in fact further removed from the experimental activation energy[12] of 30.5 kJ mol^{-1}. Thus one should be extremely careful when interpreting calculated activation energies, especially in the case of simple-level calculations, which might give the correct barrier fortuitously, as reported for the addition of the methyl radical to ethylene at the HF/3-21G level of theory.[16]

It has been found[33,34] that the QCISD(T)/6-311G** level of theory predicts a reasonably accurate barrier for the addition of the methyl radical to ethylene, and calculations at this level have been performed here in an attempt to obtain reliable activation energies for the ethyl radical to ethylene addition. Details of these calculations will be reported elsewhere[23] and only the most important results will be given here. The zero-point vibrational energy (ZPVE) correction was calculated at the HF/6-31G* level of theory as were the temperature corrections (i.e., the second term in eq 4), using a scaling factor of 0.9135 for the HF/6-31G* ZPVEs.[28,35] A value of 30.9 kJ mol^{-1} was obtained for the critical energy E_0 at the QCISD(T)/6-311G**//6-31G* level of theory. After applying a temperature correction ($+RT$) to 323 K (+1.8 kJ mol^{-1}), an activation energy of 32.7 kJ mol^{-1} was obtained. This value is in good agreement with the experimental value of 30.5 kJ mol^{-1} for the ethyl radical to ethylene addition[12] and the value of 34.3 kJ mol^{-1} (at atmospheric pressure) reported for the high-pressure polymerization of ethylene.[30]

Although the activation energies can be calculated accurately using such high-level calculations for small systems, this is not currently feasible in practice for larger monomer systems. Calculations at this level of theory are computationally demanding and require a large disk capacity. For example, the QCISD(T)/6-311G** calculation on the transition state for the ethyl radical to ethylene addition required more than 5 days of CPU time (i.e., about 2 weeks of wall clock time) and approximately 1 Gbyte of disk space on an IBM RS/6000 320H workstation. These computational requirements currently limit the applicability of the method described for obtaining accurate activation energies to moderately small molecules.

Implications of the Theory

The calculations performed in this study give considerable physical insight into the factors that influence the propagation event. In this light, the propagation of ethylene may be considered as a homopropagation reaction in which there are no substituent effects, and it is interesting to discuss in what way substituents (i.e., different monomers) can affect the frequency factor of the propagation reaction. As has been shown, the most important terms in the frequency factor to be considered here are the translational and rotational terms (particularly the internal rotations), the vibrational term being more or less a constant of order unity. For macroradicals, the translational and external rotational terms are solely due to the monomer and can be easily determined. The translational term is only dependent on the mass of the monomer and the external rotational term only on the mass and shape (moments of inertia) of the monomer. We have already seen how a consideration of the translational and rotational terms provides a rationalization of $k_p^1 > k_p$.

In the reacting radical and transition state, the partition functions for the internal rotations are determined by the geometry of the molecule and the barriers to rotation. Different conformations of the reacting molecule could have different barriers to rotation for corresponding internal rotations and hence lead to different values for the frequency factors. This is in line with the observation made for the propagating methyl methacrylate radical, where it was found that syndiotactic addition is favored over isotactic addition.[36] The important transitional modes arising as internal rotations will be less hindered for the syndiotactic orientation as compared with the isotactic orientation. Another example in the literature that can be explained with our model is the difference found between the k_p values of *cis*- and *trans*-4-*tert*-butylcyclohexyl methacrylate (BCHMA),[37] the k_p value for *trans*-BCHMA being higher than that for the *cis* isomer. Since it is not likely that there is a great difference in the respective activation energies, the main difference should arise from the frequency factors, which may be expected from the theory outlined in this paper.

Having shown that the most important internal rotations are the rotations at the radical terminus (see Figure 4), we now note that the substituents in the last (terminal) unit and the second last (penultimate) unit can influence such rotations in both the macroradical and the transition state and so affect the frequency

factor. This result is very important in free-radical copolymerization, where there has been a considerable debate about penultimate unit effects,[38] and it gives support to the existence of a significant penultimate unit effect.[39]

Futhermore, knowing that these internal rotations govern the frequency factor, the theory also explains the increased propagation rates found upon deuteration of monomers.[40,41] Due to a higher mass, the moments of inertia of the internal rotations will increase and hence the rotational partition functions for both the TS and the reactants will increase. The TS is found to be affected more, leading to a higher frequency factor. The calculation of the frequency factor for the addition of deuterated heptyl radical to deuterated ethylene confirms this: the frequency factor increases by about 16%, which is of the same order of magnitude as observed for the rate enhancements found in the styrene/deuterated styrene (28%)[40] and methyl methacrylate/deuterated methyl methacrylate (28%)[41] systems.

Our analysis suggests that it should be possible to predict that k_p value for a specific monomer if the k_p value for an electronically similar monomer (e.g., ethyl acrylate is considered to be electronically similar to methyl acrylate, and ethyl methacrylate to methyl methacrylate) has been measured accurately, simply by considering the differences in rotational and translational contributions to the frequency factor.

A last implication is that by calculating the frequency factor with the relatively simple HF/3-21G procedure, one should be able to estimate the activation energy for a specific propagation reaction if the experimental value of k_p is available at a known temperature.

Sensitivity Analysis of the Model

In the previous sections, we discussed the model that we have used to estimate the frequency factor of propagation reactions in free-radical polymerizations. It was shown that the molecular properties obtained from quantum chemical calculations that influence the calculated frequency factors are (i) the rotational constants corresponding to both internal and external rotations, (ii) the frequencies of the vibrational modes, and (iii) the low-frequency vibrations and torsions. It is of interest to examine the sensitivity of the calculated frequency factors to the accuracy of the calculation of these properties and/or the assumptions in our model.

First we examine the sensitivity with respect to the calculated rotational constants. These depend on the optimized geometry of the molecule, which in turn depends on the level of theory that is used. Comparison of the rotational constants for the internal rotations at the levels of theory that we have used in this study indicates that the differences between the different levels of theory are generally smaller than 3%, which leads to differences in the frequency factor of less than 5%. To explore this further, we considered two "worst case scenarios" for the addition of the ethyl radical to ethylene in which we decreased or increased the rotational constants by 10% (i.e., three times more than the observed differences at the three levels of theory). In the case where we increased the rotational constants in the TS by 10% and decreased the rotational constants in the ethyl radical by 10%, a decrease in the frequency factor of 15% was found (at 323 K, HF/3-21G). With the opposite changes, the frequency factor was increased by 15% (at 323 K, HF/3-21G).

For the external rotations, the products of the three principal rotational constants at the levels of theory used lie typically within 3% of one another, which leads to differences in overall contributions to the frequency factor of less than 5%. Again, the two worst case scenarios we considered involve a 10% change in opposite directions for the TS and reactants. This leads to an increase in the frequency factor of 16% in one case and a decrease of 14% in the other case. Hence, we may conclude for both the internal and external rotations that the effects of errors in the rotational constants on the calculated frequency factors are very small.

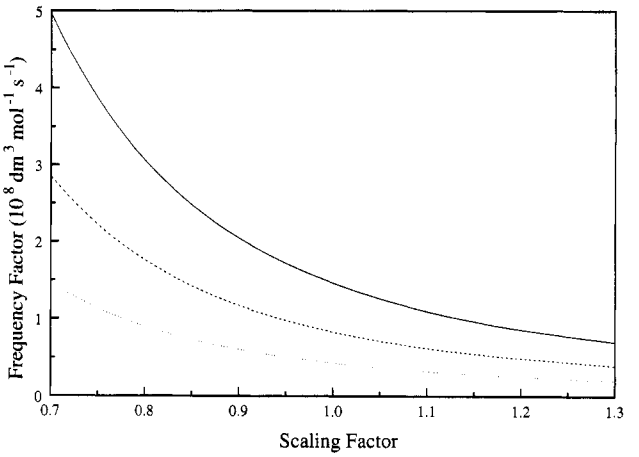

Figure 5. Dependence of the calculated frequency factor on the scaling factor for the theoretical frequencies at the HF/3-21G level of theory (323 K): (—) ethyl radical addition; (- - -) butyl radical addition; (···) heptyl radical addition.

Table 9. Comparison of Calculated Frequency Factors (10^7 dm^3 mol^{-1} s^{-1}) for *n*-Alkyl Radical Additions to Ethylene Using the Harmonic Oscillator, Hindered Rotor, and Free Rotor Approximations for the Low-Frequency Torsional Modes or Using Only the Five Real Transitional Modes of the Transition States

	frequency factor[a]			
	harmonic oscillator	hindered rotor	free rotor	transitional modes
ethyl	3.0	17.2	24.9	12.9
n-propyl	3.3	8.7	16.5	7.1
n-butyl	3.3	9.8	18.3	6.1
n-pentyl	3.3	7.9	15.2	4.9
n-hexyl	3.3	6.3	11.7	
n-heptyl	3.3	4.3	10.0	

[a] At 323 K, HF/3-21G.

Next, we examine the sensitivity with respect to the accuracy of our calculated vibrational frequencies. This is done by calculating the frequency factors for the addition of *n*-alkyl radicals to ethylene using scaling factors ranging from 0.70 to 1.30 (i.e., corresponding to underestimation and substantial overestimation of the frequencies). In Figure 5, the scaling factor dependence of the frequency factor is shown for the addition of the ethyl, butyl, and heptyl radicals and it can be seen that the frequency factor increases by a factor of 3 after scaling by the unlikely low value of 0.70. Using a scaling factor of 1.3 halves the frequency factors.

Next, we examine the effect of treating the three important low-frequency torsional modes (i.e., the methylene torsion in the radical and the ethylene and propylene torsions in the TS) as harmonic oscillators, hindered rotors, and free rotors, successively. The results are shown in Table 9 and it can be seen that the hindered rotor treatment yields results that lie between the results obtained by the harmonic oscillator and free rotor treatments.

Finally, we examine the effect of the nontransitional modes on the frequency factor by omitting all but the five real transitional modes from the vibrational and internal rotational partition functions using the hindered rotor treatment for the ethylene torsion and the harmonic oscillator approximation for the other four modes. The results for the ethyl to pentyl radical additions to ethylene are included in Table 9 and it can be seen that the contribution to the total frequency factor made by the nontransitional modes is between 3 and 9 times smaller than the contribution made by the transitional modes. In the hexyl and heptyl radical cases, it is very difficult to identify the individual transitional modes with confidence, and hence these calculations have not been performed.

It is apparent from the above discussion that the approximations in our calculations and/or model lead to individual errors that are generally quite small. It is conceivable that these all act in the same direction, in which case they would lead to an overall error in the calculated frequency factor amounting to an order of magnitude or more. However, this is not particularly likely and we would conisder that a more realistic estimate of the uncertainty inherent in frequency factors predicted by the present model to be a factor of about 1−4. For relative frequency factors, we expect the uncertainty to be significantly lower, as the uncertainties introduced in the model are of a systematic nature.

Conclusions

The theory presented in the current study yields frequency factors that are in reasonable agreement with experimental data in the literature, which indicates a satisfactory description of the physics of the propagation process. It is shown that a simple level of ab initio molecular orbital theory is sufficient for the prediction of the frequency factor, which makes it possible to use the theory for quite large monomers. The fundamental reason that satisfactory values of the frequency factor can be obtained at a simple level of ab initio molecular orbital theory is that the frequency factor is largely determined by the geometry of the rotating groups in the reactants and the transition state, and their respective rotational potentials, which are known to be predicted quite reliably by relatively simple levels of theory. Although it is possible to calculate accurate activation energies for small systems, this requires a high level of ab initio theory and is not currently possible in practice for large monomer systems because of the computational resources that are required.

Good insight is obtained into the factors that govern the frequency factor. By considering the important internal rotations, it is possible to explain several observations reported in the literature associated with substituent effects. The theory also suggests that the penultimate unit could significantly affect the frequency factor for the propagation reaction, giving support to the ideas of the penultimate unit effect in free-radical copolymerization.

Finally, we note that the theory will allow an improved interpretation of experimental data and more soundly based predictions of the behavior of different monomers.

Acknowledgment. We gratefully acknowledge useful discussions with Dr. Meredith Jordan, Dr. Gregory Russell, and Professor H. Bernhard Schlegel, the provision of the one-dimensional Schrödinger equation code by Dr. George Bacskay, the provision of an Overseas Postgraduate Research Scholarship for J.P.A.H., support by the Australian Research Council, and a generous allocation of time on the Fujitsu VP2200 supercomputer of the Australian National University Supercomputer Facility.

References and Notes

(1) (a) Buback, M.; Garcia-Rubio, L. H.; Gilbert, R. G.; Napper, D. N.; Guillot, J.; Hamielec, A. E.; Hill, D.; O'Driscoll, K. F.; Olaj, O. F.; Jiacong Shen; Solomon, D.; Moad, G.; Stickler, M.; Tirrell, M.; Winnik, M. A. *J. Polym. Sci., Polym. Lett.* **1988**, *26*, 293. (b) Buback, M.; Gilbert, R. G.; Russell, G. T.; Hill, D. J. T.; Moad, G.; O'Driscoll, K. F.; Shen, J.; Winnik, M. A. *J. Polym. Sci., Polym. Chem.* **1992**, *30*, 851. (c) Gilbert, R. G. *Pure Appl. Chem.* **1992**, *10*, 1563.
(2) Buback, M.; Gilbert, R. G.; Hutchinson, R. A.; Klumperman, B.; Kuchta, F.-L.; Manders, B. G.; O'Driscoll, K. F.; Russell, G. T.; Schweer, J. *Macromol. Chem. Phys.*, submitted for publication.
(3) Davis, T. P.; O'Driscoll, K. F.; Piton, M. C.; Winnik, M. A. *Polym. Int.* **1991**, *24*, 65.
(4) For some more recent reviews of TST, see, for example: (a) Laidler, K. J.; King, M. C. *J. Phys. Chem.* **1983**, *87*, 2657. (b) Truhlar, D. G.; Hase, W. L.; Hynes, J. T. *J. Phys. Chem.* **1983**, *87*, 2664.
(5) For a general textbook on reaction dynamics, see, for example: Gilbert, R. G.; Smith, S. C. *Theory of Unimolecular and Recombination Reactions*; Blackwell: Oxford, 1990.
(6) Guaita, M. *Makromol. Chem.* **1972**, *154*, 191.
(7) See, for example: (a) Neumark, D. M. *Acc. Chem. Res.* **1993**, *26*, 33. (b) Polanyi, J. C.; Zewail, A. H. *Acc. Chem. Res.* **1995**, *28*, 119.
(8) Burkert, U.; Allinger, N. L. *Molecular Mechanics*; ACS Monograph 177; American Chemical Society: Washington, DC, 1982.
(9) Dewar, M. J. S.; Zoebisch, E. G.; Healy, E. F.; Stewart, J. J. P. *J. Am. Chem. Soc.* **1985**, *107*, 3902.
(10) Hehre, W. J.; Radom, L.; Schleyer, P. v. R.; Pople, J. A. *Ab Initio Molecular Orbital Theory*; John Wiley & Sons: New York, 1986.
(11) See, for example: (a) Walling, C. *Free Radicals in Solution*; Wiley: New York, 1957. (b) Mill, T.; Mayo, F.; Richardson, H.; Allara, D. L. *J. Am. Chem. Soc.* **1972**, *94*, 6802. (c) Morrison, B. R.; Piton, M. C.; Winnik, M. A.; Gilbert, R. G.; Napper, D. H. *Macromolecules* **1993**, *26*, 4368.
(12) (a) Reichardt, C. *Solvents and Solvent Effects in Organic Chemistry*, 2nd ed.; VCH Publishers: Weinheim, 1988. (b) Denisov, E. T. *Liquid-Phase Reaction Rate Constants*; IFI/Plenum: New York, 1974. (c) Kerr, J. A.; Parsonage, M. J. *Evaluated Kinetic Data on Gas Phase Addition Reactions*; Butterworths: London, 1972.
(13) McQuarrie, D. A. *Statistical Mechanics*; Harper & Row: New York, 1976.
(14) For the ethyl radical, see: (a) Pacansky, J.; Gardini, G. P.; Bargon, J. *J. Am. Chem. Soc.* **1976**, *98*, 2665. (b) Pacansky, J.; Dupuis, M. *J. Am. Chem. Soc.* **1982**, *104*, 415. (c) Chettur, G.; Snelson, A. *J. Phys. Chem.* **1987**, *91*, 3488.
(15) Wilson, E. B.; Decius, J. C.; Cross, P. C. *Molecular Vibrations*; McGraw-Hill: New York, 1955.
(16) Fueno, T.; Kamachi, M. *Macromolecules* **1988**, *21*, 908.
(17) Lewis, G. N.; Randall, M. *Thermodynamics*, 2nd ed. (revised by K. S. Pitzer and L. Brewer); McGraw-Hill: New York, 1961.
(18) Pitzer, K. S.; Gwinn, D. W. *J. Chem. Phys.* **1942**, *10*, 428.
(19) Troe, J. *J. Chem. Phys.* **1977**, *66*, 4758.
(20) Truhlar, D. G. *J. Comput. Chem.* **1991**, *12*, 266.
(21) Pople, J. A.; Head-Gordon, M.; Raghavachari, K. *J. Chem. Phys.* **1987**, *87*, 5968.
(22) Frisch, M. J.; Trucks, G. W.; Head-Gordon, M.; Gill, P. M. W.; Wong, M. W.; Foresman, K. B.; Johnson, B. G.; Schlegel, H. B.; Robb, M. A.; Replogle, E. S.; Gomperts, R.; Andres, J. L.; Raghavachari, K.; Binkley, J. S.; Gonzalez, C.; Martin, R. L.; Fox, D. J.; DeFrees, D. J.; Baker, J.; Stewart, J. J. P.; Pople, J. A. *Gaussian 92, Revision D.3*; Gaussian, Inc.; Pittsburgh, PA, 1992.
(23) Heuts, J. P. A.; Gilbert, R. G.; Radom, L. Manuscript in preparation.
(24) Nordholm, S.; Bacskay, G. B. *Chem. Phys. Lett.* **1976**, *42*, 253.
(25) Bacskay, G. B. Unpublished work.

(26) Gilbert, R. G.; Jordan, M. J. T.; Smith, S. C.; Pitt, I. G.; Greenhill, P. G. *UNIMOL Program suite*, available from the authors: School of Chemistry, University of Sydney, NSW 2006, Australia, or by electronic transfer from gilbert@chem.usyd.edu.au.
(27) Pople, J. A.; Schlegel, H. B.; Krishnan, R.; DeFrees, D. J.; Binkley, J. S.; Frisch, M. J.; Whiteside, R. A.; Hout, R. F.; Hehre, W. J. *Int. J. Quant. Chem. Symp.* **1981**, *15*, 269.
(28) Pople, J. A.; Scott, A. P.; Wong, M. W.; Radom, L. *Isr. J. Chem.* **1993**, *33*, 415.
(29) (a) Scott, A. P.; Radom, L. To be published. (b) The standard scale factors for theoretical frequencies in ref 28 were evaluated using a least-squares procedure and are thus most appropriate for high frequencies. They are useful, for example, in evaluating zero-point vibrational energies. On the other hand, the most important frequencies in the present study are the low frequencies. Reexamination of the vibrational data after high-frequency vibrations have been eliminated (ref 29a) produces scale factors more appropriate for the low-frequency vibrations. On the basis of the results obtained using this latter approach, scale factors of 0.95 (HF/3-21G), 0.89 (HF/6-31G*), and 1.00 (MP2/6-31G*) have been used in the present study. The HF/3-21G scale factor has an uncertainty of about 0.03 and this in turn introduces an uncertainty in the frequency factor of about 10%.
(30) Schweer, J. Ph.D. Thesis, Göttingen University, Germany, 1988.
(31) Russell, G. T. Private communication.
(32) See, for example: (a) Deady, M.; Mau, A. W. H.; Moad, G.; Spurling, T. H. *Makromol. Chem.* **1993**, *194*, 1691. (b) Krstina, J.; Moad, G.; Solomon, D. H. *Eur. Polym. J.* **1993**, *29*, 379. (c) Moad, G.; Rizzardo, E.; Solomon, D. H.; Beckwith, A. L. J. *Polym. Bull.* **1992**, *29*, 647.
(33) Wong, M. W.; Pross, A.; Radom, L. *J. Am. Chem. Soc.* **1994**, *116*, 6284.
(34) Wong, M. W.; Radom, L. *J. Phys. Chem.* **1995**, *99*, 8582.
(35) The Arrhenius parameters were obtained by numerical differentiation of eq 1, which immediately yields the temperature correction to E_0 (i.e., the second term in eq 4, corresponding to the difference of the activation enthalpy at temperature T and at 0 K) + RT. This implies that the frequencies used in the temperature correction are scaled by a factor of 0.89 (see ref 29) and the ZPVEs are scaled by a factor 0.9135, because the high frequencies are the dominant ones here and they should be scaled for a better result. See ref 28.
(36) Tonge, M. P.; Pace, R. J.; Gilbert, R. G. *Macromol. Chem. Phys.* **1994**, *195*, 3159.
(37) Matsumoto, A.; Mizuta, K.; Otsu, T. *Macromolecules* **1993**, *26*, 1659.
(38) See, for example: (a) Bamford, C. H. *Polym. Commun.* **1989**, *30*, 36. (b) Fukuda, T.; Ma, Y.-D.; Kubo, K.; Inagaki, H. *Macromolecules* **1991**, *24*, 370. (c) Fukuda, T.; Kubo, K.; Ma, Y.-D. *Prog. Polym. Sci.* **1992**, *17*, 875.
(39) Heuts, J. P. A.; Gilbert, R. G.; Maxwell, I. A. To be submitted for publication.
(40) Wittmer, P.; Böck, H.; Naarmann, H.; Schmitt, B. J. *Makromol. Chem.* **1981**, *182*, 2505.
(41) Olaj, O. F.; Schnöll-Bitai, I. *Makromol. Chem., Rapid Commun.* **1990**, *11*, 459.

MA950597G